water

MDPI

Article

Spatiotemporal Dynamics and Explanatory Factors of Ecological Quality in the Baihetan Reservoir Drawdown Zone (2016–2025): An Expert-Guided PCA-Based Assessment Approach

Jingwei Li [1], Gan Sun [2], Jiang Yu [2], Jingying Lu [2], Xuejun Cheng [1], Ruimeng Zhou [2], Shufeng Liu [3], Wei Jin [4,5], Yuqing Wang [4,5], Yu Fang [4,5], Yijun Pan [4,5] and Chang Li [4,5,*]

[1] Space Information Technology Application Research Institute, Changjiang River Scientific Research Institute, Changjiang Water Resources Commission, Wuhan 430010, China; lijingwei@mail.crsri.cn (J.L.); chengxj@mail.crsri.cn (X.C.)
[2] China Three Gorges Construction Engineering Corporation, Chengdu 610041, China; sun_gan@ctg.com.cn (G.S.); yu_jiang@ctg.com.cn (J.Y.); lu_jingying@ctg.com.cn (J.L.); zhou_ruimeng@ctg.com.cn (R.Z.)
[3] Hubei Polytechnic Institute, Xiaogan 432000, China; liushufeng_21@163.com
[4] Key Laboratory for Geographical Process Analysis & Simulation of Hubei Province, Central China Normal University, Wuhan 430079, China; jinwei1997@mails.ccnu.edu.cn (W.J.); wangyuqing@mails.ccnu.edu.cn (Y.W.); yf@ccnu.edu.cn (Y.F.); pyj@mails.ccnu.edu.cn (Y.P.)
[5] College of Urban and Environmental Sciences, Central China Normal University, Wuhan 430079, China
* Correspondence: lcshaka@126.com or lichang@ccnu.edu.cn

Abstract

As the world's second-largest hydropower station, the reservoir drawdown zone of Baihetan Hydropower Station faces severe ecological disturbance from periodic water level fluctuations; exploring its ecological impact patterns is critical for global reservoir drawdown zone ecological restoration and assessment. Taking the drawdown zone of Baihetan Hydropower Station as the study area, an expert-guided PCA-based assessment framework is proposed: 13 key ecological indicators were screened through expert consultation to ensure ecological relevance and data reliability, followed by objective Principal Component Analysis (PCA) for indicator decorrelation, dimensionality reduction, and comprehensive scoring. Combined with spatiotemporal hot–cold spot and overlay analysis, spatially explicit ecological assessment maps were generated using multi-temporal remote sensing images (covering low-water exposure (July flood season), post-flood impoundment (November), and high-water stabilization (December) periods), spanning a continuous decade from 2016 to 2025 to construct a complete 10-year spatiotemporal cube, which include a 5 km buffer along the mainstream of the Jinsha River. Main results: (1) After the 2021 commissioning, comprehensive ecological quality declined overall, with weakened seasonal ecosystem responses, significant homogenization, and an oscillating cold spot-dominated pattern without stable high-quality hot spots. (2) Marked longitudinal differentiation existed: downstream had better, more stable ecological quality, while upstream showed declining quality and greater hot–cold spot variation associated with reservoir operation and anthropogenic disturbances. (3) Spatiotemporal active points only aggregated briefly in November, indicating autumn–winter impoundment inhibited ecological activity. (4) The first principal component explained 85.52% of variance, with VIIRS nighttime lights, wetness and NDVI as the dominant contributing indicators. The temporal changes reported here are associations with the commissioning of the hydropower station and are not presented as demonstrated causal effects. This study provides a transferable framework for the ecological assessment of hydropower-driven vulnerable areas worldwide.

Check for updates

Academic Editor: José Miguel Sánchez Pérez

Received: 23 September 2026
Revised: 22 October 2026
Accepted: 27 October 2026
Published: 9 November 2026

Copyright: © 2026 by the authors. Licensee MDPI, Basel, Switzerland. This article is an open access article distributed under the terms and conditions of the Creative Commons Attribution (CC BY) license.

Keywords: Baihetan Hydropower Station; reservoir drawdown zone; ecological environment assessment; spatiotemporal hot–cold spots; overlay analysis; Jinsha River; expert-guided PCA assessment

1. Introduction

As the world's third-longest river, the Yangtze River ranks among the top in global hydropower generation [1]. The Baihetan Hydropower Station, the world's second-largest hydropower project in the Yangtze River Basin, China, undertakes the strategic task of "West-to-East Power Transmission". However, the construction and operation of the hydropower station have inevitably impacted the local ecological environment, such as altering the surface cover and disturbing the original hydrological rhythm [2]. Moreover, previous related studies [3–5] have found that global dam construction exerts significant impacts on large river systems. The Baihetan area forms a topographic gradient zone due to the large elevation difference. Combined with the water level fluctuations caused by hydropower station regulation and seasonal changes, the reservoir water level in this area shows significant periodic fluctuations, eventually forming a large-scale and ecologically sensitive drawdown zone. At present, the laws and mechanisms of how such combined factors affect the ecological environment remain unclear, lacking systematic and comprehensive research reports. In-depth exploration of this issue is crucial for maintaining the ecological security of the Yangtze River, optimizing the layout of hydropower development, realizing the green development of hydropower projects, and promoting the coordinated and sustainable development of clean energy and the ecological environment.

With the large-scale construction of dams and hydropower projects worldwide, the drawdown zone, as a special ecological transition area between aquatic and terrestrial ecosystems, has gradually become a research hot spot [6]. From the perspective of global research progress, some countries in North America and Europe have focused on typical large reservoirs and lakeside zones, mainly exploring the interaction mechanism from the perspective of "water level regulation–vegetation structure–ecological function". Through transect monitoring and species investigation, they have initially revealed the impact of water level fluctuations on the ecological environment of drawdown zones. With the deepening of research, the research scope has been continuously expanded, the research objects have become increasingly diversified, the research content has gradually shifted from single-factor analysis to multi-process interaction, and the research scale has extended from single reservoirs to watershed and cascade reservoir systems. In recent years, China has paid increasing attention to the research on drawdown zones, especially in the Yangtze River Basin. With the completion of a number of large hydropower projects such as the Three Gorges Dam, the research on drawdown zones in the Yangtze River Basin has been in-depth, and a series of achievements have been made in the causes of environmental problems [2], ecological functions, management strategies, and vegetation reconstruction and restoration of drawdown zones.

(1) Ecological Environment Evaluation Progress for Drawdown Zones

In the development process of ecological environment evaluation methods for drawdown zones, early research mainly relied on transect monitoring and species investigation to conduct qualitative or semi-quantitative evaluation from the perspective of vegetation structure and ecological functions.

With the advancement of research, evaluation methods have been continuously enriched and improved. In terms of indicator construction, the evaluation system has gradually expanded from single vegetation indicators to a comprehensive indicator system covering

https://doi.org/10.3390/w18212786

hydrology, topography, soil, vegetation, and other dimensions. For example, hydrological indicators such as water level fluctuation amplitude, frequency, and duration, topographic indicators such as slope gradient and length, soil indicators such as soil texture and nutrient content, and vegetation indicators such as vegetation type and biomass are comprehensively considered to fully reflect the ecological environment characteristics of the drawdown zone. The proposal of the Remote Sensing Ecological Index (RSEI) [7] provides a method for assessing the quality of the ecological environment on a large scale. Recent studies have combined comprehensive assessment with explicit driver identification; for instance, by coupling a coordination degree with geographically and temporally weighted regression to simulate the interaction between human and environmental subsystems [8]. Such models require explanatory variables that are external to the composite index, and these are rarely available for data-scarce drawdown zones.

The weighting method is a key factor affecting the reliability of evaluation results. At present, commonly used weighting methods can be divided into subjective weighting methods and objective weighting methods [9–15], as below. Subjective weighting methods include the Analytic Hierarchy Process (AHP), Delphi Method, Fuzzy Analytic Hierarchy Process (FAHP), etc., which rely on expert experience and have strong ecological interpretability but are susceptible to human subjective factors. Objective weighting methods include Principal Component Analysis (PCA), Entropy Weight Method (EWM), Coefficient of Variation Method (CVM), etc., which automatically calculate weights based on data variation or correlation, avoiding subjective bias but being sensitive to data quality and distribution. Therefore, the combination of subjective and objective weighting methods has gradually attracted widespread attention. For example, the combination model based on AHP and EWM not only considers expert experience but also utilizes the objectivity of data, improving the rationality of weights. Alternatively, traditional objective weighting methods can be improved from the perspective of the mathematical principles of the method itself or the complementarity of multiple objective weighting methods, such as the improved Coefficient of Variation Method and improved Principal Component Analysis. Based on this, other analytical and prediction methods, such as regression analysis, can be carried out to further clarify the relationship between variables.

(2) Driving Forces of the Ecological Environment in Drawdown Zones

From the research in different regions of the world, the research on the driving forces of the ecological environment in drawdown zones shows different characteristics and progress. In early research regions such as Europe and North America, scholars first paid attention to the impact of water level regulation on the vegetation structure of drawdown zones. Under natural flood conditions, the vegetation in the drawdown zone has a certain adaptability and succession law. However, the water level regulation after dam construction has changed this natural rhythm, leading to the simplification of riparian community structure and association with greenness in nearby areas [16]. For example, around some large reservoirs, the communities originally dominated by perennial plants have gradually been replaced by pioneer annual plants, and the rate of community replacement has accelerated. Mechanistically, water level fluctuations affect the seed dispersal, germination, and growth processes of plants, and the differences in the adaptability of different plants to water level changes lead to changes in community structure.

With the expansion of research areas, in the research on drawdown zones of newly built reservoirs in Asia, Africa, and other regions, in addition to water level fluctuations, the impact of human activities has become increasingly prominent. In some developing countries in Asia, engineering activities such as reservoir-surrounding road construction and port and terminal development are frequent. These activities have changed the slope morphology and surface cover conditions of the drawdown zone, intensifying habitat fragmentation.

In the Yangtze River Basin, the seasonal changes in water level caused by the monsoon climate are more intense, which has a unique impact on the ecological environment of the drawdown zone. Moreover, within a large river basin, increasing rainfall intensity causes spatially divergent hydrological changes [17]. The complex water level fluctuations in the drawdown zone of the Yangtze River Basin, affected by natural seasonal changes, elevation differences, and dam operation regulation, have a profound impact on the local ecological environment. The unique topography, geomorphology, and rich biodiversity of the Yangtze River Basin make the ecological environment of the drawdown zone here show distinct characteristics. For example, frequent water level fluctuations lead to changes in the distribution pattern of animal and plant communities in the drawdown zone, and soil erosion and nutrient loss caused by water level changes have also become important issues affecting the ecological health of the drawdown zone. In addition, human activities such as agricultural planting and aquaculture in the drawdown zone of the Yangtze River Basin further complicate the driving forces of the ecological environment, making the research on the driving forces of the ecological environment in the drawdown zone of this region more challenging and important.

Despite the valuable insights provided by previous studies, several critical limitations remain to be addressed in the ecological assessment of reservoir drawdown zones:

(1) The applicability of single weighting methods in the complex ecological system of drawdown zones is limited. Although various ecological environment evaluation methods for drawdown zones have been developed, subjective weighting methods rely on expert experience and have certain subjectivity, while objective weighting methods are based on data but have high requirements on data quality and completeness. Therefore, the idea of combining subjective and objective weighting has attracted more and more attention. However, the indicators selected for evaluation are often correlated, and with the increase in indicator dimensions, it will bring great difficulties to data processing and analysis. In this case, Principal Component Analysis (PCA) has obvious evaluation advantages, as it can effectively remove the correlation between indicators and achieve dimensionality reduction, thereby simplifying the data analysis process and improving evaluation efficiency and accuracy. Nevertheless, the integration of expert-based subjective indicator screening and PCA-based objective dimensionality reduction has not been fully applied in the ecological evaluation of drawdown zones, resulting in insufficient balance between ecological interpretability and statistical rigour in existing evaluations.

(2) The research on the interaction mechanism of driving forces in drawdown zones is not in-depth enough. At present, although the research on the driving forces of the ecological environment in drawdown zones has clarified the important impact of natural and human factors, the research on the interaction mechanism between various factors and their differences in different spatiotemporal scales is still insufficient. For example, how water level fluctuations and human activities synergistically affect the ecological functions of the drawdown zone, and how this synergistic effect changes in different seasons and regions, all need further research to reveal, so as to formulate more accurate ecological protection and restoration strategies.

(3) There are obvious deficiencies in the research on exploring the spatiotemporal patterns of the ecological environment in drawdown zones using methods such as spatiotemporal hot–cold spot analysis and overlay analysis. This is reflected in two aspects: first, the overall number of studies taking drawdown zones as the special research object is limited; second, existing studies mostly focus on themes such as vegetation restoration and pollutant migration, and there are few studies that specifically use methods such as spatiotemporal hot–cold spot analysis and overlay analysis to systematically reveal the spatiotemporal evolution patterns of drawdown zones. There are few cases of in-depth

applications of such spatial statistical methods in the excavation of ecological processes in drawdown zones, and the systematic understanding of the specific connotation and formation process of drawdown zones still has room for further deepening.

To address the above research gaps, this study takes the drawdown zone of the Baihetan Hydropower Station (2016–2025) as the study area and makes the following main contributions:

(1) An expert-guided PCA-based assessment framework is proposed for the ecological environment of drawdown zones, which integrates expert consultation for indicator screening and PCA for dimensionality reduction, balancing the ecological interpretability of expert knowledge and the statistical rigour of data-driven methods. Expert consultation is first used to screen indicators, which ensures the ecological relevance and practical rationality of the evaluation system, avoiding the deviation of indicator selection caused by pure data-driven methods. On this basis, PCA is used to decorrelate and reduce the dimensionality of the selected indicators, which enhances the robustness of the evaluation results and solves the problem of multicollinearity among multi-dimensional ecological indicators. This framework seeks to balance the ecological interpretability of expert knowledge with the statistical decorrelation of data-driven methods, offering a structured and interpretable basis for the ecological assessment of complex reservoir drawdown zones.

(2) A long-time series spatiotemporal analysis approach based on the spatiotemporal cube model and hot–cold spot analysis is leveraged to the ecological assessment of drawdown zones. This approach discretizes the study area according to time and space, systematically analyzes the spatiotemporal dynamic characteristics of the ecological environment quality of the drawdown zone, and combines the analysis of influencing factors and explanatory factors to clarify the spatiotemporal evolution law of the ecological environment. This approach strengthens the integration of spatial and temporal dimensions in the ecological evaluation of drawdown zones, which helps to deeply understand the dynamic response of the drawdown zone ecosystem to natural and anthropogenic disturbances.

2. Materials and Methods

2.1. Study Area

The core study area is the reservoir area of the Baihetan Hydropower Station, as well as a 5 km buffer zone along both banks of the mainstream of the Jinsha River. As shown in Figure 1, the broader lower Jinsha River cascade corridor spans approximately 101°30′ E to 104°30′ E and 26°00′ N to 29°00′ N, located at the eastern edge of the Hengduan Mountains, with a typical deeply incised valley landform, steep bank slopes, large topographic fluctuations, and a fragile ecological environment background. The climate belongs to the dry–hot valley type, characterized by concentrated precipitation and strong evaporation, which exacerbates the risk of soil and water loss in the area. Within this corridor, the domain used for indicator extraction, PCA and spatiotemporal mapping is discretized into a raster of 3220 × 1687 pixels at a 30 m spatial resolution, corresponding to an extent of approximately 96.6 km by 50.6 km. Their map frame spans 102°46′ E to 103°54′ E and 26°10′ N to 27°52′ N, and the 30 m analysis raster described above is contained within this frame. All indicator extraction, PCA and spatiotemporal statistics were computed solely on the raster cells located inside the 5 km buffer mask, and no result is reported outside that raster.

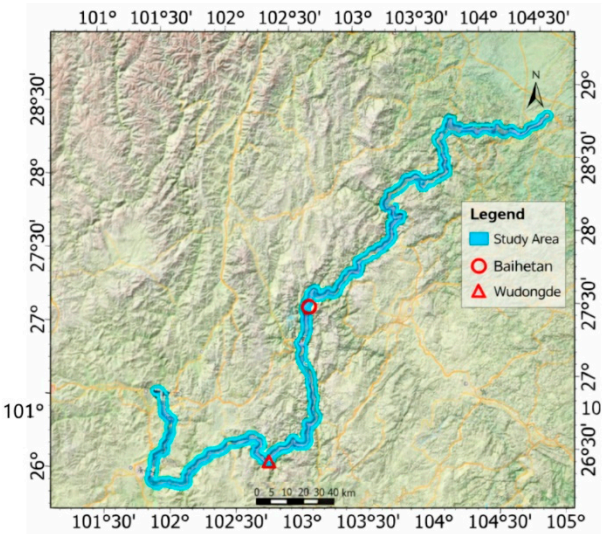


Figure 1. Study area.

The designed annual average runoff at the dam site of the Baihetan Reservoir shows obvious seasonal distribution characteristics: the runoff within the year is mainly concentrated in the flood season (June–October), accounting for more than 70% of the annual runoff, while the runoff in the non-flood season (November–May of the next year) accounts for a small proportion. After the impoundment and operation of the hydropower station, the water level of the reservoir area follows the "winter storage and summer release" regulation mode. After the flood season (around October), the reservoir gradually impounds water toward its normal pool level, so the water level continues to rise through late autumn and winter; it then recedes from the high level before the next flood season (around May to June), thus periodically exposing large areas along the reservoir banks, namely the drawdown zone.

This special zone has experienced repeated alternations from aquatic to terrestrial environments, becoming a focus and a difficult area where ecological degradation and restoration processes are intensely intertwined, and natural succession and artificial restoration measures interact. The 5 km buffer zone is designated to fully cover the ecologically sensitive areas directly and indirectly affected by reservoir water level fluctuations, ensuring the scientificity and completeness of the study scope. The strict drawdown zone, that is, the elevation band between the normal pool level of 825 m and the dead water level of 765 m, covers about 96.6 square kilometres in the Baihetan Reservoir [18]. The 5 km buffer analyzed in this study is wider than that band and covers the belt affected both directly and indirectly by the water level fluctuation, and the results are reported for this wider belt.

2.2. Data Sources and Preprocessing

To comprehensively, dynamically, and accurately capture the spatiotemporal changes in ecological parameters in this area, this study systematically collected and processed multi-source and multi-temporal remote sensing data from 2016 to 2025. The main data include Landsat 8/9 OLI/TIRS images of the U.S. Landsat programme, Sentinel-2 MSI Level-2 surface reflectance products and Moderate Resolution Imaging Spectroradiometer (MODIS) products. These data sources complement each other in spatiotemporal resolution and spectral characteristics: Landsat data provides a medium–high spatial resolution basis for the calculation of key ecological parameters, while MODIS products provide continuous time series for the acquisition of parameters such as Gross Primary Productivity (GPP). To ensure the spatial comparability of all indicator data, resampling technology was used to unify all derived data to a 30 m spatial resolution with the projected coordinate system

WGS 1984 UTM Zone 47N. This scale can balance the efficiency of large-scale analysis and the depiction of ground object details in the drawdown zone. Remote sensing retrieval of water constituents has reached high spatial resolution even in optically complex inland waters [19,20], which supports the use of water-related indicators in the assessment. In the time dimension, the study spans the complete decade from 2016 to 2025 and samples three representative months each year, namely July, November and December, to maintain a consistent seasonal observation window across the pre-impoundment baseline (2016–2020, reflecting the natural wet-season versus dry-season hydrological regime prior to initial reservoir filling in April 2021) and the post-commissioning operational period (2021–2025). Because daily measured water level logs were not available to the authors, the hydrological phases of these three months during the post-commissioning period were referenced against the published operational regime of the Baihetan Reservoir [18,21], which specifies a normal pool level of 825 m, a flood-limited water level of 785 m and a dead water level of 765 m, yielding an annual vertical fluctuation band of about 60 m. Under this operational schedule, the reservoir recedes toward its lowest drawdown level in late May to early June, operates at a relatively low level under flood-season regulation in July, impounds water after the flood season to reach and maintain the 825 m normal pool level through autumn (including November), and transitions into high-water stabilization and initial winter water-supply drawdown in December. Accordingly, among the three sampled months in the post-commissioning period, July represents the flood-season low-water exposure phase, when the upper part of the elevation band between the flood-limited and normal pool levels is subaerially exposed, although it does not capture the brief pre-flood drawdown minimum near the dead water level in late May and early June; November represents the post-impoundment high-water inundation phase near the normal pool level; and December represents the winter high-water stabilization and early supply phase. Because this three-month sampling does not include the late-May and early-June drawdown minimum and relies on published operational schedules rather than daily gauge records, the phase assignment is approximate, as acknowledged in Section 4.5. Based on this, 13 key ecological environment indicators from Table 1 were extracted and calculated, including Gross Primary Productivity (GPP, reflecting vegetation carbon sequestration capacity), soil erosion modulus (reflecting soil and water loss intensity), Land Surface Temperature (LST, reflecting thermal environment), and Normalized Difference Vegetation Index (NDVI), constructing a comprehensive evaluation index system covering three dimensions: ecological vitality, environmental pressure, and topographic and socio-economic impacts. The study leveraged continuous observed data spanning the complete 10-year period from 2016 to 2025 to robustly construct the spatiotemporal cube required for hot spot analysis.

Table 1. Overview of multi-source remote sensing datasets, derived ecological indicators, and auxiliary parameters.

Category	Subcategory	Specific Indicators (Code)	Native Resolution	Sources and Retrieval Basis	Coordinate System
Ecosystem and Environmental Status	Climatic and Thermal Factors	Precipitation (xi1, auxiliary for RUSLE); Wetness (WET, xi2); Land Surface Temperature (LST, xi3)	0.1 degree/30 m/30 m	China National Meteorological Data, ERA5-Land and GLDAS, and Landsat 8/9 OLI/TIRS (Tasselled Cap Wetness and thermal bands)	WGS84

Table 1. *Cont.*

Category	Subcategory	Specific Indicators (Code)	Native Resolution	Sources and Retrieval Basis	Coordinate System
	Topographic Factors	Slope Gradient and Slope Length (xi4, auxiliary for RUSLE)	12.5 m	ALOS PALSAR Digital Elevation Model (DEM)	WGS84
	Vegetation Factors	FVC (xi5), NDVI (xi6), EVI (xi7), SAVI (xi8), GVI (xi9)	30 m/250 m	Landsat 8/9 OLI, Sentinel-2 MSI Level-2 products, and MODIS vegetation index series (MOD13)	WGS84
	Hydrological/Water Index	NDWI (xi16)	30 m	Sentinel-2 MSI and Landsat 8/9 OLI Level-2 surface reflectance (calculated from green and near-infrared bands)	WGS84
	Soil Factors	Soil Erosion Intensity (RUSLE, xi12, tons per hectare per year)	1000 m	Calculated via the Revised Universal Soil Loss Equation (RUSLE) using multi-source fused inputs	WGS84
Human Survival Security and Anthropogenic Pressure	Anthropogenic Disturbance	Nighttime Lights (NTL, xi13); NDBI (xi17)	500 m/30 m	NPP-VIIRS Nighttime Lights data; Sentinel-2 and Landsat 8/9 Level-2 reflectance (NDBI calculated from shortwave infrared and near-infrared bands)	WGS84
	Productivity Indicators	NPP (xi14), GPP (xi15)	500 m	MODIS NPP/GPP products (MOD17 series) and CASA light-use efficiency inversion	WGS84
	Land Cover (Auxiliary Input)	Ecosystem Classification, Land Use/Cover (auxiliary for RUSLE and CASA)	10 m/30 m	Sentinel-2 and Landsat OLI classification products	WGS84

Note: All 13 core PCA indicators (xi2, xi3, xi5 to xi9, xi12 to xi17) and the auxiliary layers were resampled onto a common 30 m analysis grid (WGS 1984 UTM Zone 47N). Continuous variables were resampled by bilinear interpolation, and categorical auxiliary variables (ecosystem classification and land use/cover, which parameterize RUSLE and CASA rather than entering PCA directly) by nearest-neighbour assignment. Resampling unifies the analysis grid and does not add native spatial information to coarser products; indicators derived from RUSLE (1000 m), NPP/GPP and nighttime lights (500 m), and MODIS products (250 m) are therefore interpreted at the meso-scale rather than at the individual pixel level.

2.3. Evaluation Framework and Spatiotemporal Analysis Methods

2.3.1. Overall Technical Framework

This study focuses on the comprehensive evaluation of the ecological environment of the drawdown zone in July, November, and December from 2016 to 2025. The technical framework is shown in Figure 2, with the following key steps: first, preprocess multi-modal remote sensing data to ensure data quality; second, based on the expert-guided PCA assessment framework, construct the evaluation indicator system through expert consultation, perform indicator normalization, and calculate the comprehensive ecological score using PCA variance contribution rates as weights; finally, construct a spatiotemporal cube model to conduct spatiotemporal hot–cold spot analysis and overlay analysis. In the data preprocessing stage, multi-source remote sensing data are systematically processed to eliminate

noise and ensure data consistency; in the indicator system construction and comprehensive score calculation link, PCA is used to concentrate information and reduce dimensionality, and PCA variance contribution rates are used as weights to ensure the objectivity of the score. Spatiotemporal hot–cold spot analysis and overlay analysis comprehensively reveal the characteristics and changes in the ecological environment in the drawdown zone.

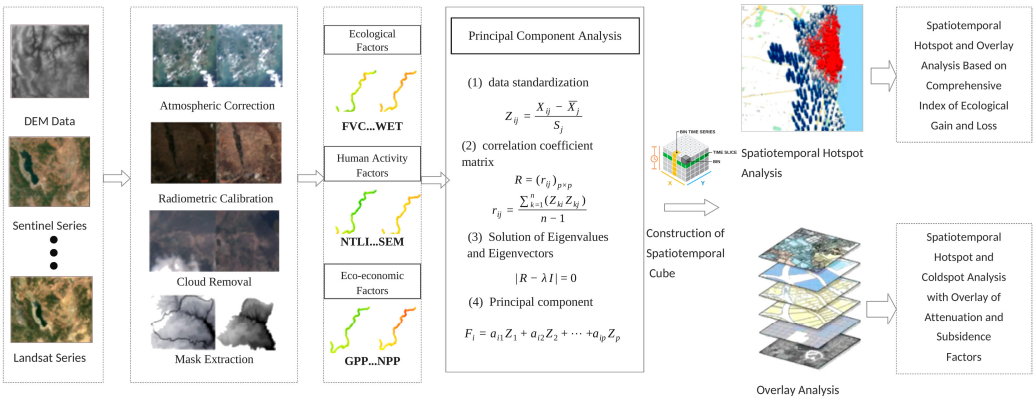


Figure 2. Technical route.

2.3.2. Data Preprocessing

The data in this study are mainly from multi-source remote sensing data such as the Sentinel series and Landsat series. Specifically, Level-2 surface reflectance products of Sentinel-2 and Landsat 8/9 were directly obtained, which have already undergone radiometric calibration and atmospheric correction by the data providers. The specific preprocessing steps include the following two aspects: (1) Cloud removal: Use cloud detection algorithms to identify and remove cloud-covered areas in the images; for pixels covered by clouds, interpolation or other reasonable processing is performed according to the information of surrounding pixels to restore or approximately restore surface information. (2) Mask extraction: Corresponding vector masks were generated according to the boundary of the study area and applied to the preprocessed remote sensing images to extract the target domain and exclude external interference. Crucially, the spatial analysis mask is kept fixed across the entire 2016–2025 period rather than being dynamically redrawn for each observation date according to the instantaneous water line. Fixing the spatial mask ensures that inter-annual and seasonal comparisons reflect genuine changes in ecological parameters over a consistent geographical domain, avoiding the confounding spatial-scale effect that would arise if the number and location of evaluated pixels changed at every time step.

2.3.3. Comprehensive Ecological Quality Assessment

Indicator Classification and Normalization

First, a multi-dimensional and hierarchical ecological environment evaluation indicator system for the drawdown zone is constructed, covering three categories of indicators: ecological and environmental status, human survival security, and ecological economy in Table 2. As a key component of the assessment framework, the indicator system was examined by a panel of eight specialists before the final list was fixed: five specialists in ecological environment assessment and three researchers in hydropower engineering ecology. The panel included specialists from the China University of Mining and Technology and from a research institute of the Chinese Academy of Sciences, and Professor Youchuan Wan, former Dean of the School of Remote Sensing and Information Engineering of Wuhan University. Each specialist evaluated the candidate indicator framework (derived from the project technical implementation plan) against a ten-point suitability benchmark (above

8 points for retention) considering ecological relevance, data availability, and scientific validity, and provided signed written review opinions endorsing the overall indicator scheme and technical route. Because the archived consultation records consist of panel-agreed written review forms and the finalized candidate table rather than individual item-by-item score sheets, inter-rater agreement cannot be retrospectively quantified with a formal statistic such as Kendall's coefficient of concordance (W); this is acknowledged as a limitation in Section 4.5. Of the candidate indicators, 13 with the highest ecological relevance and the most complete data coverage were retained for PCA. Two candidate indicators were excluded: the Perpendicular Vegetation Index (PVI), which is largely redundant with NDVI and SAVI and requires a soil line that cannot be reliably parameterised in the study area, and soil organic matter content, whose available product has incomplete spatial coverage over the Jinsha River valley and is a static multi-year average without inter-annual variation, so it cannot enter a ten-year time series. Two further candidate variables, precipitation and slope gradient and length, were not discarded: they enter the assessment as the rainfall erosivity (R) and topographic (LS) factors of RUSLE and are therefore represented through the soil erosion indicator rather than as separate indicators, which avoids collinearity with RUSLE. Second, according to ecological significance, the original indicators are clearly divided into positive indicators and negative indicators. Positive indicators such as GPP and NDVI indicate better ecological conditions with higher values; negative indicators such as soil erosion modulus and nighttime lights data indicate greater ecological pressure with higher values. Normalization is performed on positive and negative indicators respectively to eliminate the impact of different indicator dimensions, and the formula is as follows: Indicators with an unfavourable ecological meaning, namely nighttime lights, soil erosion intensity, LST and NDBI, were normalized in the reverse direction, so that a high normalized value denotes a favourable ecological condition for every indicator. After this step, all indicators enter the retained component with a positive loading, and a high composite score therefore corresponds to better ecological conditions.

From an ecological mechanism perspective, the 13 retained indicators are structured into five functional groups representing interconnected processes in the drawdown zone: (i) vegetation vigour and structural coverage, represented by NDVI, EVI, SAVI, FVC, and GVI; (ii) surface moisture and thermal regimes, captured by WET, NDWI, and LST; (iii) topographic susceptibility and soil erosion pressure, integrated by RUSLE (which incorporates precipitation erosivity and slope gradient and length); (iv) ecosystem carbon fixation and productivity, quantified by NPP and GPP; and (v) anthropogenic disturbance and impervious surface expansion, characterized by VIIRS nighttime lights and NDBI. Indicators within each group intentionally share partial covariance to capture the same ecological process from complementary spectral angles, while the subsequent PCA step orthogonalizes these correlated variables to remove redundancy.

$$r_{ij} = \begin{cases} \frac{x_{ij} - min(x_{ij})}{max(x_{ij}) - min(x_{ij})} & (Positive\ indicators) \\ \frac{max(x_{ij}) - x_{ij}}{max(x_{ij}) - min(x_{ij})} & (Negative\ indicators) \end{cases} \quad (1)$$

where x_{ij} represents the value of the j-th indicator in the i-th region of the sample, and r_{ij} is the normalized value. Data normalization ensures that all indicators are in the same comparable scale, laying a foundation for subsequent PCA and weighting calculation.

Table 2. Candidate ecological indicators screened by the expert consultation panel and their selection status.

Category	Subcategory	Candidate Indicators (Code)	Data Source and Retrieval Method	Status in Final PCA (13 Retained)
Ecosystem and Environmental Status	Climatic and Thermal Factors	Precipitation (xi1), Wetness (WET, xi2), LST (xi3)	National Meteorological Data, ERA5-Land, and Landsat/Sentinel Tasselled Cap and thermal bands	Retained: xi2, xi3 (xi1 integrated via the RUSLE R-factor)
	Topographic Factors	Slope Gradient and Slope Length (xi4)	ALOS PALSAR Digital Elevation Model (12.5 m)	Integrated via the RUSLE LS-factor
	Vegetation Factors	FVC (xi5), NDVI (xi6), EVI (xi7), SAVI (xi8), GVI (xi9), PVI (xi10)	Landsat 8/9 OLI, Sentinel-2 MSI, and MODIS MOD13 series	Retained: xi5 to xi9 (xi10 excluded due to collinearity and soil-line uncertainty)
	Soil Factors	Soil Organic Matter Content (xi11)	National Tibetan Plateau Data Center	Excluded (static multi-year average with incomplete valley coverage)
	Hydrological/Water Index	NDWI (xi16)	Sentinel-2 MSI and Landsat 8/9 OLI surface reflectance	Retained: xi16
Human Survival Security and Anthropogenic Pressure	Environmental Risk and Anthropogenic Pressure	Soil Erosion Intensity (RUSLE, xi12), Nighttime Lights (xi13), NDBI (xi17)	RUSLE model calculation, NPP-VIIRS data, and Landsat/Sentinel shortwave infrared and near-infrared reflectance	Retained: xi12, xi13, xi17
	Productivity Indicators	NPP (xi14), GPP (xi15)	MODIS MOD17 series and CASA light-use efficiency inversion	Retained: xi14, xi15

Note: Exactly 13 continuous indicators (xi2, xi3, xi5, xi6, xi7, xi8, xi9, xi12, xi13, xi14, xi15, xi16, xi17) were retained for the final PCA. Precipitation (xi1) and slope gradient and length (xi4) enter the assessment as the rainfall erosivity (R) and topographic (LS) factors of RUSLE (xi12) rather than as separate PCA inputs, which avoids structural collinearity. PVI (xi10) and soil organic matter content (xi11) were excluded for the reasons detailed in Section Indicator Classification and Normalization.

Principal Component Analysis (PCA)

Principal Component Analysis (PCA) is a data dimensionality reduction and information concentration technology based on statistical characteristics. Its core principle is to transform a set of possibly correlated original variables into a set of linearly uncorrelated new variables (i.e., principal components) through orthogonal linear transformation. These principal components are arranged in descending order of variance, where the first principal component retains the largest proportion of variation information in the original data, and subsequent components capture the largest part of the remaining variation in turn. The specific steps are as follows: Prior to PCA, the Kaiser–Meyer–Olkin (KMO) measure of sampling adequacy was computed as 0.782, and Bartlett's test of sphericity was significant ($p < 0.001$), confirming that the indicator dataset was suitable for dimensionality reduction. The analysis was implemented in Python 3.8.5 with block-wise (incremental) computation over all valid pixels of the 30 time steps and a single loading matrix shared by all periods, which avoids the memory limit of conventional statistical packages and, more importantly,

keeps the composite scores comparable across years and seasons. Extreme values were screened before the components were computed, and pixels with a missing value in any indicator were excluded from the corresponding time step.

Note that the standardized variables used to construct the correlation matrix and to extract the eigenvectors are obtained from the direction-aligned min–max-normalized indicators, and the pixel-wise component scores used for mapping are projected from the same direction-aligned layers, so that positive composite scores directly reflect favourable ecological conditions. Minor negative values (down to −0.1488 in Figure 3) occur only where low values on the first component coincide with negative loadings on the secondary components (PC2 and PC3).

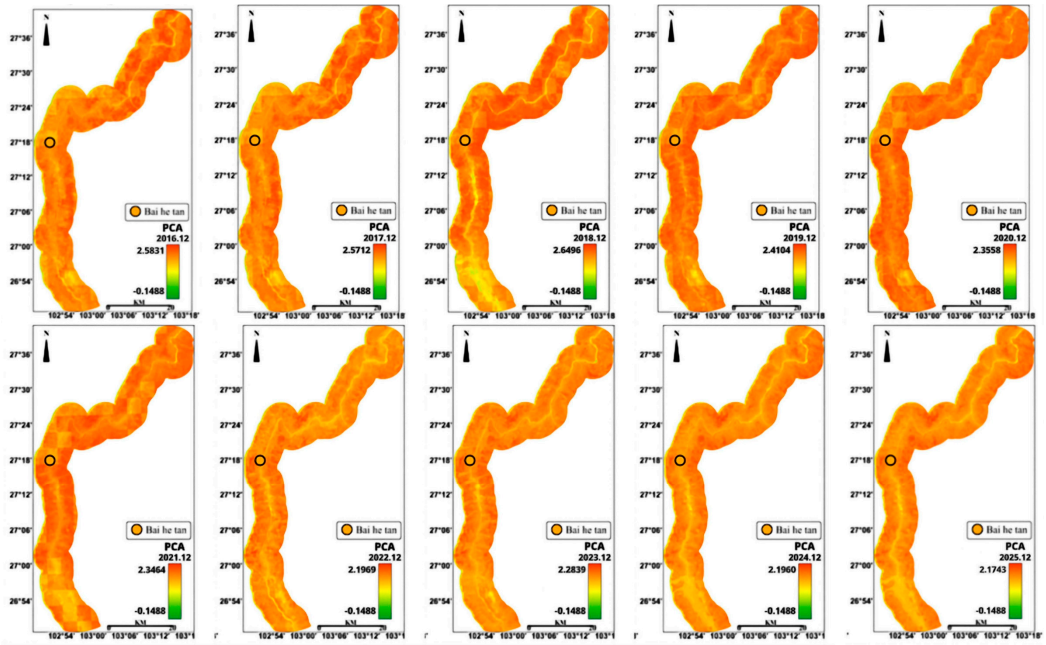


Figure 3. Spatiotemporal distribution of comprehensive ecological quality scores (2016–2025). The score is a dimensionless weighted combination of the retained components, so only its relative magnitude is meaningful and only differences among pixels and periods are interpreted.

First, data standardization is performed to eliminate the impact of dimension differences, and the formula is as follows:

$$z_{ij} = \frac{x_{ij} - \overline{x_j}}{s_j} \tag{2}$$

where x_{ij} is the value of the j-th indicator in the i-th region; $\overline{x_j}$ and s_j are the mean and standard deviation of the j-th indicator, respectively.

Second, construct the correlation coefficient matrix:

$$R = \left(r_{ij}\right)_{p \times p} \tag{3}$$

$$r_{jk} = \frac{1}{n-1} \sum_{i=1}^{n} z_{ij} z_{ik} \tag{4}$$

where R is the correlation coefficient matrix, n is the number of samples, and p is the number of indicators. Here, z_{ij} and z_{ik} denote the standardized values of indicators j and k, respectively; the Pearson correlation coefficient matrix is computed based on standardized variables to ensure dimension-free comparability.

Third, solve the eigenvalues λ_1,λ_2,...,λ_p and eigenvectors a_1,a_2,...,a_p by solving the characteristic equation:

$$|R - \lambda I| = 0 \tag{5}$$

Fourth, the principal component expression is:

$$F_i = a_{i1}Z_1 + a_{i2}Z_2 + \cdots + a_{ip}Z_p \tag{6}$$

where F_i is the i-th principal component, and a_{ij} is the eigenvector coefficient.

Fifth, calculate the principal component contribution rate and cumulative contribution rate:

$$\alpha_i = \frac{\lambda_i}{\sum_{k=1}^{p} \lambda_k} \tag{7}$$

$$\beta_m = \frac{\sum_{i=1}^{m} \lambda_i}{\sum_{k=1}^{p} \lambda_k} \tag{8}$$

where β_m is the cumulative variance contribution rate of the first m principal components. The cumulative contribution rate is usually taken as $\beta_m \geq 85\%$ to ensure that most of the information of the original indicators is retained.

Finally, the comprehensive score is calculated by weighted summation of the principal components using the contribution rate as the weight:

$$F = \sum_{i=1}^{m} \alpha_i F_i \tag{9}$$

Determination of Comprehensive Weights and Calculation of Scores

To objectively determine the weight of each principal component in the final evaluation, the variance contribution rate of each principal component derived from PCA is directly used as its weight, which reflects the explanatory power of each component for the original ecological indicators. Based on this weight, the comprehensive ecological environment score of each pixel in July, November, and December of each year from 2016 to 2025 is calculated, providing a quantitative basis for subsequent spatiotemporal analysis.

2.3.4. Spatiotemporal Analysis Methods

Spatiotemporal Hot–Cold Spot Analysis

Using the spatiotemporal cube, the study area is discretized according to time and space to construct a spatiotemporal cube model. Taking each spatiotemporal unit as the analysis object, spatial hot–cold spots are detected using the Getis-Ord Gi* statistic, which is a commonly used spatial autocorrelation index for identifying the spatial agglomeration pattern of high and low values. When the Getis-Ord Gi* statistic is positive and passes the significance test ($p < 0.05$), it is considered that the high values of the comprehensive score are aggregated in space, i.e., hot spot areas; when the Getis-Ord Gi* statistic is negative and passes the significance test ($p < 0.05$), it is considered that the low values of the comprehensive score are aggregated in space, i.e., cold spot areas. The spatial weight matrix adopts a binary contiguity scheme with a distance threshold d set to 600 m. This distance equals 20 pixels on the 30 m grid and approximates the width of a bank segment of the drawdown zone, so that every unit has enough neighbours for a stable estimate while the neighbourhood remains local enough to resolve bank-scale clustering. Statistical significance is assessed via 999 permutations at the 95% confidence level. The threshold only controls how many neighbours are accumulated into each local sum, so changing it changes the size and the number of the detected clusters rather than the temporal behaviour on which the oscillating category is defined: a larger threshold merges neighbouring units into fewer and

larger significant clusters, whereas a smaller threshold yields more fragmented clusters and more units with too few neighbours to be tested. A significant cold spot indicates that low values cluster in relative terms within the study area, and it is not interpreted as absolute ecological degradation. The specific calculation method of the Getis-Ord Gi* statistic is as follows [22]:

Let Q_i represent the sum of squared weights:

$$Q_i = \sum_{j=1}^{n} ij_2^w \tag{10}$$

$$i_*^G(d,t) = \frac{\sum_{j=1}^{n} w_{ij}(d) S_{j,t} - \overline{X_t} W_i}{\sigma_t \sqrt{\frac{nQ_i - i_2^W}{n-1}}} \tag{11}$$

where $S_{j,t}$ represents the observed value (comprehensive ecological score) at position j in time step t; w_{ij} represents the spatial weight matrix, defining the neighbourhood relationship between positions i and j (adaptive distance threshold d is set according to the study area); $\overline{X_t}$ and σ_t represent the global mean and standard deviation of the comprehensive score in time step t, respectively.

(1) $S_{j,t}$ is the core connection point between the formula and the drawdown zone indicator system: all quantitative indicators of the drawdown zone can be directly used as its values, and the spatiotemporal quantitative values of each indicator correspond to the observed values in different time and space units, becoming the core data basis for hot–cold spot analysis.

(2) Spatial weight variables such as $w_{ij}(d)$ are adapted to the spatial characteristics of the drawdown zone: such variables set the distance threshold d and adjacent relationship according to the geographical spatial scope of the drawdown zone (such as shoreline division, elevation gradient, grid unit), define the weight rules for the spatial agglomeration analysis of each indicator of the drawdown zone, and their values are determined by the spatial unit division method of the drawdown zone, serving the calculation of spatial correlation.

(3) Statistical characteristic variables such as $\overline{X_t}$ and σ_t reflect the overall spatiotemporal level of the drawdown zone indicators: $\overline{X_t}$ is the mean value of a certain indicator of the drawdown zone in all spatial units within time t, and σ_t is the corresponding standard deviation. Both are calculated based on the observed values of the specific indicators of the drawdown zone, which are used to standardize the results to eliminate the impact of indicator dimension differences on the determination of hot–cold spots in the drawdown zone.

(4) The calculation result of $i_*^G(d,t)$ represents the spatiotemporal agglomeration pattern of the drawdown zone indicators: by substituting each indicator of the drawdown zone, combined with the spatial weight and statistical characteristic variables, the calculated value directly reflects the spatiotemporal hot–cold spot distribution of the indicator in the drawdown zone (e.g., areas with high vegetation coverage are hot spots of vegetation indicators, and areas with strong soil erosion are hot spots of erosion indicators).

$i_*^G(d,t)$ In the equations above, Q_i denotes the sum of squared spatial weights and W_i the sum of spatial weights connected to unit i, where w_ij(d) is the binary spatial weight between units i and j defined by the distance threshold d = 600 m; G_i*(d, t) is the Getis-Ord statistic of unit i at time step t, computed from the observed composite score of the neighbouring units together with the global mean and standard deviation of the composite score at that time step.

Overlay Analysis

The identified spatiotemporal hot–cold spot maps of comprehensive scoring are accurately overlaid using GIS overlay analysis, and overlay analysis is carried out for the same

region of the study area at different times, specifically divided into July–November overlay analysis and July–December overlay analysis. Through overlay analysis, the changes in spatiotemporal hot–cold spots on the time scale are evaluated, and the conversion relationship between different hot–cold spot types (e.g., from hot spot to cold spot, from oscillating cold spot to persistent cold spot) is clarified. Combined with the comprehensive score of the ecological environment of the drawdown zone in the study area and the spatiotemporal hot–cold spot distribution in specific months, the dynamic changes in the ecological environment of the drawdown zone are judged, providing a scientific basis for the precise management and decision-making of the ecological environment of the drawdown zone.

3. Results

3.1. Principal Component Analysis and Comprehensive Scoring Results

3.1.1. Principal Component Analysis Results

PCA was performed on the 13 retained ecological indicators across all valid 30 m pixels within the 5 km buffer corridor of the Baihetan Reservoir, covering 30 time steps, that is, three representative months per year (July, November and December) from 2016 to 2025, with a spatial extent of 3220 × 1687 pixels at a 30 m resolution. Within this workflow, domain-relevant indicators were first screened through expert consultation and subsequently orthogonalized via PCA to reduce dimensionality and remove multicollinearity. Principal Component Analysis was implemented in Python 3.8.5 rather than in a conventional statistical package: all valid pixels of the 30 time steps were pooled and fitted once with a single shared loading matrix using block-wise (incremental) computation, which overcomes memory limits and keeps the composite scores comparable across periods. The core results are as follows:

(1) Variance explanation rate: PC1 achieved an eigenvalue of 11.118, accounting for 85.52% of the total variance (13.000), which satisfies both the Kaiser criterion (eigenvalue above 1) and the 85% cumulative variance threshold on its own. PC2 (eigenvalue 0.833) and PC3 (eigenvalue 0.283) explained 6.41% and 2.18% of the variance, respectively, bringing the cumulative explained variance of the first three components to 94.11%, whereas each remaining component explained less than 2%. In the deeply incised valley of the study area, hydrothermal conditions, vegetation vigour, topographic erosion and human activities co-vary closely across space and time. This strong intrinsic multicollinearity among the 13 input variables explains why a single dominant axis (PC1) captures 85.52% of the total variance, motivating the use of PCA to orthogonalize overlapping ecological information into an uncorrelated composite index.

(2) Indicator loading coefficients and normalized importance ratio: Based on the mathematical logic of PCA, the dominant contributing indicators of the ecological quality of the drawdown zone in this study were clarified. The larger the absolute value of the loading coefficient of the principal component, the stronger the contribution and interpretability of the indicator to the principal component. Among them, nighttime lights (0.482), wetness (0.421), and NDVI (0.346) with loading coefficients > 0.3 were the dominant indicators. The normalized importance ratio is a standardized weight reflecting the weight ratio of the indicator among all input variables. The higher the value, the greater the comprehensive impact on ecological quality. In this analysis, the normalized importance exceeding 10% were nighttime lights (23.203%), wetness (17.721%), and NDVI (11.958%), and the cumulative normalized importance of the three indicators exceeded 50%. The normalized importance was calculated as I_j = a_j1^2/sum(a_j1^2) over the 13 indicators, where a_j1 is the loading of indicator j on the first principal component; because the loading vector has unit length, the denominator equals one, so I_j reduces to a_j1^2. These percentages refer to the first principal component only, which explains 85.52% of the total variance, whereas PC2 and

PC3 explain 6.41% and 2.18%. Because the indicators with an unfavourable ecological meaning were normalized in the reverse direction, all loadings on the retained component are positive and a high composite score corresponds to better ecological conditions. Among them, the human activity intensity characterized by nighttime lights data is a potential anthropogenic pressure factor and a dominant indicator associated with the ecological quality of the drawdown zone. The screening of these core indicators through prior expert consultation ensured that the dominant indicators identified by PCA are consistent with the actual ecological characteristics of the drawdown zone, avoiding the deviation of indicator importance caused by pure data-driven analysis.

(3) Restoration direction: As shown in Table 3, the ecological restoration of the drawdown zone in this area should take the three indicators of nighttime lights, wetness, and NDVI as the core targets, focusing on the design of restoration around human survival activities, shoreline humidity conditions, vegetation coverage and growth vitality. Other secondary influencing indicators can be used as auxiliary verification dimensions for restoration effects and are not included in the core design content of the restoration plan; in addition, a dynamic monitoring, anthropogenic disturbance control and phased management and acceptance system centred on the three indicators can be established to form a closed-loop management of restoration around the dominant contributing indicators identified by PCA, ensuring that the restoration work is targeted to the core impact logic of the ecological quality of the drawdown zone. Linking the restoration targets to the top-loading indicators allows spatial management priorities to remain consistent with the primary dimensions of variation in the composite index.

Table 3. PCA loadings and normalized importance of the 13 retained ecological indicators.

Indicator Name	Abbreviation/Code	PC1 Loading Coefficient	Normalized Importance Ratio
VIIRS Nighttime Lights	NTL (xi13)	0.482	23.20%
Tasselled Cap Wetness	WET (xi2)	0.421	17.72%
Normalized Difference Vegetation Index	NDVI (xi6)	0.346	11.96%
Normalized Difference Water Index	NDWI (xi16)	0.273	7.45%
Green Vegetation Index	GVI (xi9)	0.265	7.03%
Soil Erosion Intensity (RUSLE)	RUSLE (xi12)	0.250	6.26%
Fractional Vegetation Cover	FVC (xi5)	0.225	5.08%
Soil-Adjusted Vegetation Index	SAVI (xi8)	0.216	4.67%
Enhanced Vegetation Index	EVI (xi7)	0.210	4.41%
Gross Primary Productivity	GPP (xi15)	0.202	4.08%
Net Primary Productivity	NPP (xi14)	0.197	3.88%
Land Surface Temperature	LST (xi3)	0.172	2.95%
Normalized Difference Built-up Index	NDBI (xi17)	0.114	1.31%
Total (PC1: eigenvalue 11.118, 85.52% of variance)	13 Retained Indicators	-	100.00%

Note: The normalized importance ratio is computed as the squared PC1 loading divided by the sum of the squared PC1 loadings over the 13 retained indicators; because the eigenvector has unit length the denominator equals one, so the ratio reduces to the squared loading. These percentages refer to the first principal component only, which explains 85.52% of the total variance.

3.1.2. Comprehensive Scoring of Ecological Environment Quality

Following indicator screening and PCA dimensionality reduction, comprehensive ecological quality scores were calculated using the variance contribution rates of the retained components as weights. From the dimensions of temporal evolution and spatial distribution, taking Baihetan Hydropower Station as the core, combined with the hydrological process of the drawdown zone in the reservoir area, the common characteristics of ecological quality evolution were sorted out in Figure 3.

(1) In the temporal distribution dimension, the ecological quality of the drawdown zone and the downstream of the Baihetan Hydropower Station showed a clear phased evolution law. From 2016 to 2020 (the pre-impoundment baseline period, prior to the initiation of reservoir filling in April 2021), the overall PCA composite score around Baihetan Hydropower Station remained in a high range, with peak scores across all three hydrological phases (July, November, and December) concentrated in this stage. During this stage, although the ecological quality of the drawdown zone showed fluctuations with the hydrological rhythm, it remained stable overall without significant degradation. The year 2021 marked a key transitional point corresponding to initial impoundment and commissioning. After 2021, the overall PCA comprehensive score of each month in the reservoir area showed a continuous downward trend, and the score in July 2025 dropped to 2.0302, the lowest value during the observation period; at the same time, the differences in ecological responses of the drawdown zone in different seasons were significantly reduced, and the seasonal characteristics that the ecological quality in the flood season (July) was relatively better than that of the dry season (November and December) gradually weakened, and the drawdown zone in the reservoir area showed an obvious trend of ecological homogenization. This phased shift coincided with the official commissioning of the Baihetan Hydropower Station in 2021 and the transition to its "winter storage and summer release" operational schedule; the correspondence reported here represents a statistical association rather than a demonstrated causal effect. The observations from 2022 to 2025 are essential for this interpretation: they show that the lower scores persisted for four years after impoundment, so the post-2021 pattern reflects a sustained shift rather than a single-year fluctuation. The composite score is a dimensionless weighted combination of the retained components, with the variance contribution of each component as the weight; its absolute value carries no physical unit and only relative differences among pixels and periods are interpreted.

To formally quantify the temporal trend reported above, a non-parametric Mann–Kendall trend test was applied to the annual mean composite score over the 2016–2025 record ($n = 10$). The test yielded a statistically significant downward trend ($S = -43$, $Z = -3.76$, two-sided $p < 0.001$), with a Sen's slope estimate of approximately -0.058 score units per year, confirming that the observed decline represents a systematic shift rather than random inter-annual fluctuation. To further evaluate the post-commissioning response, we compared the pre-impoundment baseline period (2016–2020; mean = 2.484, SD = 0.092) with the post-commissioning operation period (2022–2025; mean = 2.146, SD = 0.051), excluding the transitional impoundment year 2021. The mean composite score decreased by 0.338 units (13.6%) between the two periods, and this reduction was statistically significant (Welch's *t*-test, $t = 6.98$, two-sided $p < 0.001$; exact Mann–Whitney U test, $U = 0$, one-sided $p = 0.008$, two-sided $p = 0.016$), with a large standardized effect size (Cohen's $d = 4.38$). Furthermore, the intra-annual score range across the three sampled hydrological phases, defined as the difference between the July and December scores, narrowed significantly from a pre-impoundment mean of 0.142 (SD = 0.031) for 2016–2020 to 0.054 (SD = 0.019) for 2022–2025 (Welch's *t*-test, $p < 0.01$), providing quantitative support for the weakened inter-phase variation among the three sampled months.

We emphasize that these statistical results establish a robust temporal association between reservoir commissioning and the observed ecological decline, but do not by themselves constitute causal attribution. Climatic variability, precipitation trends, land-use change, and regional vegetation dynamics over the same decade cannot be fully disentangled from the hydropower effect based on temporal coincidence alone. The attribution to Baihetan operation should therefore be interpreted as a working hypothesis supported by the phased change pattern and the response of the dominant indicators (nighttime lights,

wetness and NDVI), rather than a definitive causal claim. A formal attribution analysis controlling for climatic and land-use covariates is recommended in future work.

(2) In the spatial distribution dimension, the spatial differentiation characteristics of the ecological environment quality in the upstream and downstream of Baihetan Hydropower Station were significant, showing an overall pattern of "better in the north and worse in the south". From the spatial visualization results of the comprehensive PCA score, the areas with relatively good ecological conditions are mainly concentrated in the downstream of Baihetan Hydropower Station. The proportion of high-value areas with high ecological quality in this area is significantly higher than that in the upstream of Baihetan Hydropower Station, and the fluctuation range of ecological quality in this area between different years and seasons is relatively gentle, with a more stable ecological state; the low-value areas with relatively poor ecological conditions are mainly concentrated in the upstream. Although the overall ecological quality of the upstream is slightly different from that of the downstream, the low-value areas are more significant. With the increase in years, the gap in ecological quality scores between the north and south of the reservoir area gradually narrowed, and the spatial heterogeneity of the overall ecological quality of the basin decreased significantly, showing a global trend of convergence in ecological quality. This spatial differentiation is associated with the combined influence of valley topography, reservoir hydrological regulation, and local human activity intensity.

3.1.3. Spatiotemporal Hot–Cold Spot Analysis Results

Overall spatiotemporal pattern of Figure 4: The spatiotemporal pattern was absolutely dominated by oscillating cold spots, while other types of hot and cold spots were only sporadically distributed in patchy patterns. The distribution of spatiotemporal hot–cold spots only showed minor variations with seasonal changes, and the overall pattern remained stable. In July, there were no concentrated high-ecological-quality hot spots across the entire reservoir area. Except for the oscillating cold spots that dominated the whole region, there was no concentrated distribution of newly emerged or intensified cold spots in both upstream and downstream areas. The overall ecological quality of the drawdown zone was at a low level, with a stable cold spot pattern. In November, no concentrated hot spot areas were formed in the reservoir area; only a very small number of hot spots appeared in the local eastern area of the Baihetan Hydropower Station, and hot spot types were almost completely absent in other regions. For cold spots, the dominant pattern of oscillating cold spots in the upstream and downstream remained unchanged. Only a small number of cold spot type changes occurred in the upstream, with no large-scale transition of cold spots to intensified or persistent types, and no significant shrinkage of the cold spot range in the downstream. In December, hot spots dissipated, and oscillating cold spots still accounted for absolute dominance. The hot spots in the local eastern area of the Baihetan Hydropower Station were converted into newly emerged cold spots. The number and scope of cold spots in the upstream did not shrink significantly, and the overall hot–cold spot pattern of the whole region returned to a stable state similar to that in July, with no large-scale expansion or contraction. The stable cold spot-dominated pattern indicates that low composite scores persisted in relative terms over most of the drawdown zone, which is consistent with the comprehensive score results. Because a significant cold spot marks the relative clustering of low values within the study area, this pattern is reported as an indication of a persistent low-value state rather than as a direct measurement of ecological degradation.

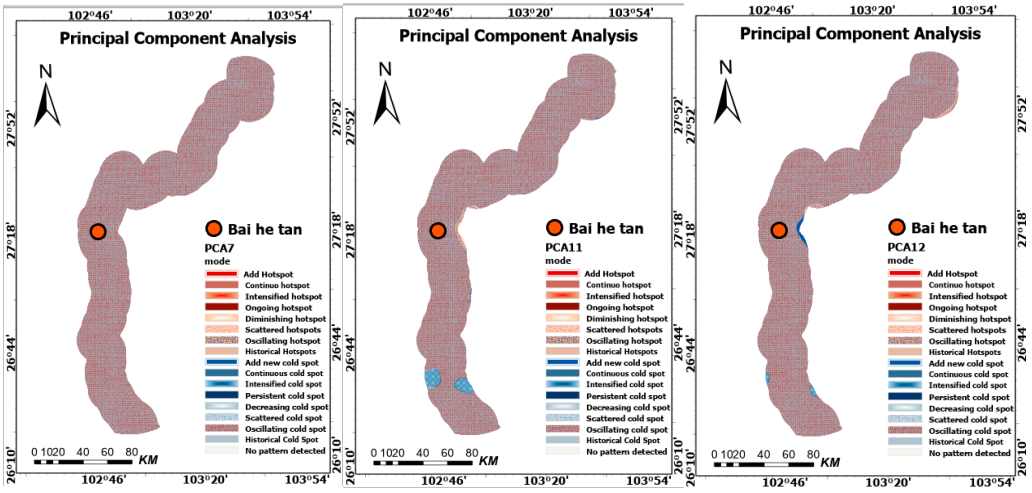


Figure 4. Spatiotemporal hot–cold spot patterns in July, November, and December (2016–2025). A hot spot is a spatial cluster of high composite scores and a cold spot a spatial cluster of low composite scores, both significant at the 95% confidence level under 999 permutations. A category is described as new, persistent or oscillating according to whether the clustering appears only in the last part of the study period, remains present through most of it, or alternates between significant and non-significant over the 30 time steps. The three panels are arranged in chronological order from left to right (July, November, December).

3.1.4. Overlay Analysis Results

(1) For the Baihetan drawdown zone between July and November in Figure 5: The whole region was dominated by oscillating cold spot areas, and areas with changes in hot–cold spot types were only sporadically distributed in a punctate pattern, mainly concentrated in the eastern part of the Baihetan Hydropower Station and local upstream areas. There were almost no areas with hot–cold spot type changes in the downstream of the reservoir area. Overall, there was no large-scale conversion of hot–cold spot types, and the spatial dominant pattern of oscillating cold spots remained unchanged. This indicates that the ecological environment of the drawdown zone has strong temporal stability in the transition from flood season to post-flood impoundment, and the response to hydrological changes is relatively gentle.

(2) For the Baihetan drawdown zone between July and December in Figure 5: The whole region was still absolutely dominated by oscillating cold spot areas. Compared with the July–November overlay analysis, the scope of areas with changes in hot–cold spot types was narrowed, with only a sporadic distribution in the upstream, downstream and very local areas around the dam site. The proportion of oscillating cold spot areas in the whole region was further increased, and the stability of the overall spatial pattern of hot–cold spots was stronger. This phenomenon is related to the gradual stabilization of the water level in the drawdown zone in December, and the ecosystem tends to a relatively stable (but low-quality) state, which further reflects the long-term fragile characteristics of the ecological environment of the drawdown zone.

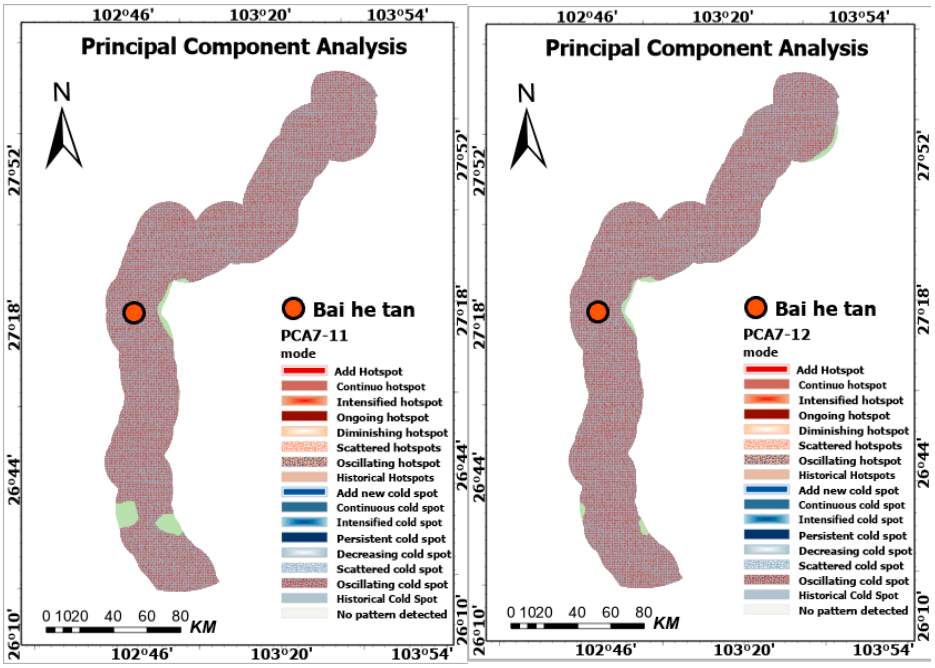


Figure 5. Overlay analysis of spatiotemporal hot–cold spot transitions between seasons. The overlay compares the category assigned to each unit in July with the category assigned to the same unit in November (July to November) and in December (July to December), so the maps show where a unit changed categories between the two phases and where it did not.

4. Discussion

4.1. Longitudinal Drawdown Pattern and Ecological Differentiation

The spatial differentiation of ecological quality and hot–cold spot patterns along the Baihetan Reservoir corridor exhibits a clear longitudinal gradient with distinct upstream–downstream characteristics [23]. The comprehensive ecological environment score of the drawdown zone around the Baihetan Hydropower Station showed an overall downward trend after the reservoir officially began impoundment in April 2021, and the station was commissioned later that year. From the perspective of the spatiotemporal hot–cold spot distribution pattern, the types of hot–cold spots around the station and across the reservoir area remained basically stable during the three key hydrological periods (July, November and December), always dominated by oscillating cold spots. No obvious high-ecological-quality hot spot agglomeration areas were formed, and no significant upgrading or large-scale conversion of cold spot types occurred. The overlay analysis results showed that, whether in the July–November or July–December period comparison, the drawdown zone of the Baihetan Reservoir was dominated by oscillating cold spot areas. Only a small range of areas with hot–cold spot type changes existed in the upstream zone of the hydropower station, and the scope of such changes tended to narrow over time, with no large-scale conversion of hot–cold spot types.

From the perspective of spatial differentiation, the downstream of the Baihetan Hydropower Station had relatively better ecological quality, with gentle fluctuations in ecological quality between different seasons, and no significant phased changes in the ecological state of the drawdown zone, while the upstream reservoir area showed a declining trend in ecological quality. Overall, the observed ecological fluctuations across the reservoir corridor show a close spatiotemporal correspondence with the periodic water level regime under station regulation, alongside the dry–hot valley climate and local human activities. In addition, potential time lags in ecosystem response may also contribute to these multi-year

patterns. Rather than claiming statistical superiority over alternative weighting methods, which would require formal quantitative benchmarking, the expert-guided PCA workflow constructed in this study is intended as a practical, interpretable compromise that pairs domain-informed indicator screening with objective statistical decorrelation, offering a transferable framework for assessing similar data-scarce reservoir corridors. A comparison between the periods before and after commissioning cannot by itself separate the effect of regulation from the other changes that took place over the same decade. Inter-annual variability of precipitation and temperature, land-use change in the surroundings of the reservoir, construction activity during the impoundment period and the regional trend of vegetation may all have contributed to the observed decline, and the data available to us do not allow these explanations to be ranked against each other. The decline is therefore reported as an association with the commissioning of the station rather than as its demonstrated consequence.

4.2. Seasonal Changes Pattern of the Ecological Environment

The inter-phase variations in the ecological environment around the Baihetan Hydropower Station reflect the combined influence of the natural hydrological rhythm and regulated reservoir operation. In the periods of July–November and July–December, the hot–cold spot types in the drawdown zone around the Baihetan Hydropower Station were always dominated by oscillating cold spots, with no obvious agglomeration areas of newly emerged or persistent hot spots. Although the comprehensive ecological quality score showed a downward trend, there was no drastic change in the spatial pattern of hot–cold spots. This characteristic is related to its location in the downstream cascade: although the regulation range of water level drop and impoundment recovery after the flood season is affected by cascade regulation, the rhythm of exposure and inundation of the drawdown zone is relatively gentle. Vegetation growth and ecological restoration did not form concentrated hot spot areas, and there was no significant hot spot expansion or cold spot upgrading. The attenuated inter-phase variation coincides with the transition from a natural hydrological regime to regulated operation, which is consistent with the pattern of ecological homogenization [24] reflected in the composite scoring results.

4.3. Dominant Contributing Indicators of Ecological Environment Changes

(1) Natural dimension: The seasonal wet–dry rhythm shaped by uneven precipitation distribution in the Jinsha River Basin forms the natural background of the drawdown zone ecosystem. Strong evaporation and distinct dry–wet seasons in the valley influence surface wetness (WET), which emerged as the second-largest contributing indicator on PC1 and represents a key environmental correlate of vegetation status. Seasonal variations in precipitation and bank-zone moisture are closely associated with indicators of vegetation vigour such as NDVI and GVI. Meanwhile, slope runoff during concentrated rainfall events is associated with heightened soil erosion intensity (RUSLE), which co-varies with vegetation and moisture conditions across the steep valley slopes. Prior expert screening ensured that these interconnected natural processes were represented in the composite index before statistical dimensionality reduction.

(2) Anthropogenic dimension: Human activities during the construction and operational phases of the Baihetan Hydropower Station represent a primary anthropogenic explanatory factor associated with the observed ecological patterns. Following the commissioning of the station in 2021, the PCA composite score in the reservoir corridor showed a statistically significant decline. Local human activities, such as shoreline development, road infrastructure, and agricultural cultivation proxied by VIIRS nighttime lights and NDBI, co-occur with hydrological regulation and are associated with increased habitat

fragmentation across the buffer zone. Furthermore, while localized ecological restoration projects coincide with sporadic improvements in NDVI and WET, these isolated hot spots remain surrounded by oscillating cold spots, suggesting that localized interventions have not yet shifted the broader regional baseline.

4.4. Restoration Recommendations

(1) Priority restoration areas: First, the upstream (southern) area of the Baihetan Hydropower Station reservoir area. The PCA comprehensive score of this area has been at a low level in the whole reservoir area for a long time, and the spatiotemporal hot–cold spot pattern is dominated by persistent oscillating cold spots, with the ecosystem in a long-term low-quality steady state. Overlay analysis shows that this area has the largest variation range of hot–cold spot types, which is the core area affected by the superposition of hydrological regulation and local anthropogenic disturbance, and is suggested by the spatial analysis as the primary area for ecological restoration. Second, the eastern area around the dam site of the Baihetan Hydropower Station, which is directly affected by the project construction and operation regulation of the power station, with the weak anti-interference ability of the ecosystem, is suggested as a key restoration area. These priority restoration areas are delineated based on the spatial clustering of low composite scores identified by our assessment framework. The field effectiveness of prioritizing these zones has not yet been established and needs to be verified through pilot projects.

(2) Restoration strategies: Guided by the dominant contributing indicators identified in the PCA (nighttime lights, wetness, and NDVI) and building upon established bio-engineering practices from regional restoration planning, targeted management measures can be spatially prioritized across the Baihetan Reservoir corridor. First, to address surface moisture limitations reflected by wetness (WET, the second-largest contributing indicator on PC1), soil water-retaining matrix amendments and seasonal supplementary irrigation can be prioritized to improve bank-zone moisture retention. Second, to address low vegetation vigour reflected by NDVI (the third-largest contributing indicator), elevation-zoned planting of native flood- and drought-tolerant pioneer species can be implemented according to inundation duration to enhance fractional cover and greenness (GVI). Third, regarding anthropogenic disturbance proxied by nighttime lights (the top contributing indicator) and NDBI, strict shoreline zoning and disturbance controls are recommended within the priority restoration zones. In addition, flexible ecological revetments and slope conservation works can be targeted at high-erosion segments identified by RUSLE, while pond-wetland conservation and ecological ditches can support shoreline water connectivity (NDWI). Rather than representing newly invented engineering techniques, our contribution here lies in using the spatial assessment and indicator weights to guide where and along which ecological dimensions these established measures should be prioritized; their actual restoration performance in the Baihetan drawdown zone remains to be tested in pilot areas before wider application.

4.5. Limitations and Future Work

Several limitations of this study should be acknowledged. First, the analysis focused on three key months (July, November, December) representing critical hydrological phases; future work could incorporate monthly or higher-temporal-resolution data to capture more nuanced seasonal dynamics. Second, the assessment framework relies on expert consultation for initial indicator screening; while this ensures ecological relevance, future studies could incorporate larger expert panels and formal consistency testing (e.g., Kendall's coefficient of concordance) to further strengthen the robustness of indicator selection. Third, ground-truth validation with field survey data would enhance the reliability of remote-

sensing-based ecological quality assessments. Finally, while field-scale Unmanned Aerial Vehicle (UAV) photogrammetry is often recommended for the ground-truth validation of remote-sensing-based ecological assessments, its application was strictly prohibited in this study. The Baihetan Hydropower Station, as critical national infrastructure, is legally designated as a strict no-fly zone for civilian UAVs. Furthermore, the massive spatial extent of the 5 km buffer zone along the mainstream renders localized, fragmented UAV flights spatially unrepresentative for capturing the regional ecological non-stationarity. Three further limitations should be noted. First, the indicator system was fixed by a panel review and the individual score sheets were not retained, so the agreement among panel members could not be quantified with a formal statistic such as Kendall's coefficient of concordance. Second, daily measured water levels of the reservoir were not available and the three observation months were assigned to hydrological phases from the published operation schedule [18,21], so the assignment is approximate. Third, the assessment rests on three months per year and on remote sensing indicators without field plots, and its design compares periods before and after commissioning; the changes reported here are therefore associations and cannot be read as causal effects of reservoir operation. Water quality parameters retrieved from high-resolution observations, such as chromophoric dissolved organic matter [19] and suspended particulate matter [20], could be added in future work to characterize the aquatic phase of the drawdown zone independently.

Fourth, because usable satellite scenes and cloud cover vary across years and months, the monthly composites rely on spatial interpolation over cloud-masked pixels, which introduces local uncertainty. Fifth, while resampling unifies all layers onto a 30 m grid, we did not re-run the entire assessment at coarser native resolutions (250 m or 500 m), nor did we perform formal leave-one-out indicator elimination, alternative weighting sensitivity tests, or quantitative benchmarking against an unfiltered PCA-only baseline. Although the dominance of meso-scale indicators suggests that the broad spatial patterns would remain stable under spatial aggregation, these sensitivity analyses, together with independent validation against high-resolution environmental monitoring records, remain important directions for future work.

5. Conclusions

This study focuses on the comprehensive evaluation of the ecological environment and its spatiotemporal patterns in the drawdown zone of the Baihetan Hydropower Station reservoir area. To address the limitations of single subjective or objective evaluation methods in the ecological assessment of drawdown zones, this study constructs an expert-guided PCA assessment framework. Subsequently, by constructing a spatiotemporal cube model combined with GIS tools, in-depth spatiotemporal hot–cold spot analysis and overlay analysis were carried out to identify the distribution of hot–cold spots of the ecological environment quality of the drawdown zone in spatiotemporal dimensions, quantitatively evaluate the changes in ecological quality in different regions and time scales, and comprehensively reveal the spatiotemporal dynamic characteristics of the ecological environment in the drawdown zone. The results illustrate how the proposed framework combines domain-informed indicator selection with statistical dimensionality reduction.

The results show that the eastern area around the dam site of the Baihetan Hydropower Station and both sides of the upstream main channel of the reservoir area generally have low PCA comprehensive scores of ecological quality, forming low-value silent areas (cold spot areas) with continuously poor ecological quality. These areas should be taken as the key targets of ecological restoration. The spatial differentiation of ecological quality between upstream and downstream is significant, showing a pattern of "better in the north and worse in the south", and the overall ecological quality shows a downward trend after

2021, with obvious ecological homogenization and a long-term fragile state dominated by oscillating cold spots.

The spatiotemporal variations in ecological quality in the study corridor reflect the combined influence of natural and anthropogenic factors. Among natural factors, periodic water level fluctuations and seasonal hydrothermal regimes are closely associated with variations in surface wetness (WET) and vegetation status (NDVI). In terms of anthropogenic factors, the transition to the "winter storage and summer release" operational schedule coincided with sustained environmental pressure across the drawdown zone, while shoreline development and engineering activities proxied by nighttime lights were associated with localized habitat fragmentation. By integrating expert indicator screening with PCA decorrelation, this study provides a practical reference for monitoring similar reservoir corridors. As emphasized throughout, the trends reported above represent statistical associations derived from remote sensing indicators and should not be interpreted as demonstrated causal effects of hydropower operation.

Future research should further enrich the evaluation method system and introduce more scoring models to improve the accuracy and reliability of evaluation results. At the same time, in-depth research on the mechanism of driving forces of the ecological environment in the drawdown zone should be strengthened, especially to explore the interaction mechanism between various factors and their functional differences at different spatiotemporal scales, so as to provide a solid theoretical basis for formulating more accurate ecological protection and restoration strategies. In addition, constructing an integrated comprehensive evaluation and management framework that comprehensively considers natural processes and engineering restoration effects will help to comprehensively and systematically evaluate the ecological environment status of the drawdown zone and promote the sustainable development of the drawdown zone ecosystem. Through continuous optimization of evaluation methods and management strategies, it is expected to better solve the global ecological restoration problems of drawdown zones, and contribute to maintaining of the ecological security of the Yangtze River and promoting the green development of hydropower projects.

Author Contributions: Conceptualization, J.L. (Jingwei Li) and C.L.; methodology, J.L. (Jingwei Li), G.S. and C.L.; software, J.L. (Jingwei Li) and J.Y.; validation, J.L. (Jingwei Li), J.Y., J.L. (Jingying Lu) and S.L.; formal analysis, J.L. (Jingwei Li) and X.C.; investigation, J.L. (Jingwei Li), G.S. and R.Z.; resources, C.L., W.J. and Y.W.; data curation, J.L. (Jingwei Li), J.Y. and Y.F.; writing—original draft preparation, J.L. (Jingwei Li); writing—review and editing, C.L., G.S. and Y.P.; visualization, J.L. (Jingwei Li) and X.C.; supervision, C.L.; project administration, C.L. and G.S.; funding acquisition, C.L., W.J. and Y.W. All authors have read and agreed to the published version of the manuscript.

Funding: This work was supported by the Scientific Research Project of China Three Gorges Construction Engineering Corporation, grant numbers JGGJ0424016 and JGGJ0424017; the Science Popularization and Education Project of Sanjiangyuan National Park in 2024, grant number QHBX-2025-31 Package Four; the National Natural Science Foundation of China (NSFC), grant numbers 41771493 and 41101407; and the Fundamental Research Funds for the Central Universities, grant numbers CCNU25JCPT001 and CCNU22QN019.

Data Availability Statement: The remote sensing data used in this study are publicly available from the U.S. Geological Survey (USGS) for Landsat imagery (https://earthexplorer.usgs.gov/), the National Aeronautics and Space Administration (NASA) for MODIS products (https://ladsweb.modaps.eosdis.nasa.gov/), and the Earth Observation Group for VIIRS nighttime lights data (https://eogdata.mines.edu/products/vnl/, accessed on 26 October 2026). The ALOS PALSAR DEM is available from the Japan Aerospace Exploration Agency (JAXA). The processed ecological quality datasets and analysis code generated during this study are available from the corresponding author upon reasonable request. The PCA loading matrix, the normalized importance of the 13 indicators and the analysis scripts are available from the corresponding author upon reasonable request.

Acknowledgments: The authors are grateful for the comments and contributions of the editors, anonymous reviewers and the members of the editorial team.

Conflicts of Interest: Author Gan Sun, Jiang Yu and Ruimeng Zhou were employed by the company China Three Gorges Construction Engineering Corporation. The authors declare that this study received funding from China Three Gorges Con-struction Engineering Corporation. The funder was not involved in the study design, collection, analysis, interpretation of data, the writing of this article or the decision to submit it for publication.

Abbreviations

AHP: Analytic Hierarchy Process; DEM: Digital Elevation Model; EVI: Enhanced Vegetation Index; FAHP: Fuzzy Analytic Hierarchy Process; FVC: Fractional Vegetation Cover; GPP: Gross Primary Productivity; GVI: Green Vegetation Index; LST: Land Surface Temperature; MODIS: Moderate Resolution Imaging Spectroradiometer; NDBI: Normalized Difference Built-up Index; NDVI: Normalized Difference Vegetation Index; NDWI: Normalized Difference Water Index; NPP: Net Primary Productivity; PCA: Principal Component Analysis; PVI: Perpendicular Vegetation Index; RUSLE: Revised Universal Soil Loss Equation; SAVI: Soil-Adjusted Vegetation Index; WET: Wetness component of Tasselled Cap Transformation.

References

1. Grill, G.; Lehner, B.; Thieme, M.L.; Geenen, B.; Tickner, D.; Antonelli, F. Mapping the world's free-flowing rivers. *Nature* **2019**, *569*, 215–221. [CrossRef] [PubMed]
2. Li, R.; Huang, H.; Zhao, H. Eco-environmental impacts of dams in the Yangtze River Basin, China. *Sci. Total Environ.* **2021**, *774*, 145743. [CrossRef] [PubMed]
3. Nilsson, C.; Reidy, C.A.; Dynesius, M.; Revenga, C. Fragmentation and flow regulation of the world's large river systems. *Science* **2005**, *308*, 405–408. [CrossRef] [PubMed]
4. Vörösmarty, C.J.; McIntyre, P.B.; Gessner, M.O.; Dudgeon, D.; Prusevich, A.; Green, P.; Glidden, S.; Bunn, S.E.; Sullivan, C.A.; Liermann, C.R.; et al. Global threats to human water security and river biodiversity. *Nature* **2010**, *467*, 555–561. [CrossRef] [PubMed]
5. Best, J. Anthropogenic stresses on the world's big rivers. *Nat. Geosci.* **2019**, *12*, 7–21. [CrossRef]
6. Abrahams, C. The ecology and management of drawdown zones. *Br. Wildl.* **2006**, *17*, 395–402.
7. Xu, H. A remote sensing index for assessment of regional ecological changes. *China Environ. Sci.* **2013**, *33*, 889–897.
8. Wang, J.; Yu, Z.; Zhang, F.; Ahmed, Z.; Johnson, V.C.; Pei, Y.; Ma, X. Exploring the interaction mechanism between urbanization and eco-environment carrying capacity in underdeveloped areas: A case study of Xinjiang, China. *J. Clean. Prod.* **2025**, *513*, 145738. [CrossRef]
9. Alqahtani, F.M.; Noman, M.A. An Integrated Fuzzy Delphi and Fuzzy AHP Model for Evaluating Factors Affecting Human Errors in Manual Assembly Processes. *Systems* **2024**, *12*, 479. [CrossRef]
10. Dou, F.; Li, X.; Yuan, F.; Lu, Z.; Li, X.; Xing, H.; Ge, W. 3D Geological Suitability Evaluation for Urban Underground Space Development Based on Combined Weighting and Improved TOPSIS. *Nat. Resour. Res.* **2022**, *31*, 693. [CrossRef]
11. Krishnan, A.R.; Kasim, M.M.; Hamid, R.; Ghazali, M.F. A Modified CRITIC Method to Estimate the Objective Weights of Decision Criteria. *Symmetry* **2021**, *13*, 973. [CrossRef]
12. Wang, J.; Zhang, L.; Chen, W.; Liu, X. A comparative analysis of the principal component analysis and entropy weight methods to establish the indexing measurement. *PLoS ONE* **2022**, *17*, e0262261. [CrossRef] [PubMed]
13. Žižović, M.; Miljković, B.; Marinković, D. Objective methods for determining criteria weight coefficients: A modification of the CRITIC method. *Decis. Mak. Appl. Manag. Eng.* **2020**, *3*, 149–161. [CrossRef]
14. Lolli, F.; Balugani, E.; Ishizaka, A.; Gamberini, R. CRITID: Enhancing CRITIC with advanced independence testing for robust multi-criteria decision-making. *Sci. Rep.* **2024**, *14*, 25094. [CrossRef] [PubMed]
15. Geng, J.; Yu, K.; Xie, Z.; Zhao, G.; Ai, J.; Yang, L.; Yang, H.; Liu, J. Analysis of Spatiotemporal Variation and Drivers of Ecological Quality in Fuzhou Based on RSEI. *Remote Sens.* **2022**, *14*, 4900. [CrossRef]
16. Fan, P.; Cho, M.S.; Lin, Z.; Ouyang, Z.; Qi, J.; Chen, J.; Emilio, F. Recently constructed hydropower dams were associated with reduced economic production, population, and greenness in nearby areas. *Proc. Natl. Acad. Sci. USA* **2022**, *119*, e2108038119. [CrossRef] [PubMed]
17. Wu, Y.; Yin, X.; Zhou, G.; Bruijnzeel, L.A.; Dai, A.; Wang, F.; Gentine, P.; Zhang, G.; Song, Y.; Zhou, D. Rising rainfall intensity induces spatially divergent hydrological changes within a large river basin. *Nat. Commun.* **2024**, *15*, 823. [CrossRef] [PubMed]

18. Zhou, B.; Deng, Y.; Zhang, Y.; Zhong, R. Spatial distribution of water level fluctuating zones in the lower Jinsha River cascade reservoirs. *J. Yunnan Univ. Nat. Sci. Ed.* **2023**, *45*, 1048–1055. (In Chinese)
19. Li, Z.; Chen, C.; Cao, N.; Jiang, Z.; Liu, C.; Oke, S.A.; Jim, C.; Zheng, K.; Zhang, F. High spatial resolution inversion of chromophoric dissolved organic matter (CDOM) concentrations in Ebinur Lake of arid Xinjiang, China: Implications for surface water quality monitoring. *Int. J. Appl. Earth Obs. Geoinf.* **2024**, *132*, 104022. [CrossRef]
20. Feng, Z.; Zhang, F.; Cai, X.; Liu, C.; Wu, D.; Zhu, Z.; Ahmed, Z.; Yuan, S.; Ma, X.; Wei, L.; et al. Quantitative inversion of suspended particulate matter in Ebinur lake, an arid region: Evidence based on radiative transfer mechanism model. *J. Hydrol. Reg. Stud.* **2025**, *61*, 102714. [CrossRef]
21. Wang, J.; Chen, H.; Xiao, L.; Li, Z. Stability and motion characteristics of bridge slope in the large reservoir area. *Hydrogeol. Eng. Geol.* **2024**, *51*, 130–139. (In Chinese) [CrossRef]
22. Cao, Z.; Wu, M.; Wang, D.; Wan, B.; Jiang, H.; Tan, X.; Zhang, Q. Space-time cube uncovers spatiotemporal patterns of basin ecological quality and their relationship with water eutrophication. *Sci. Total Environ.* **2024**, *916*, 170195. [CrossRef] [PubMed]
23. Liu, Y.; Huang, G.; Zhai, M.; Wang, N.; Fu, Y.; Pan, X. Unveiling long-term indirect socio-economic and environmental effects of large-scale hydropower project. *Sci. Total Environ.* **2025**, *959*, 178317. [CrossRef] [PubMed]
24. Poff, N.L.; Olden, J.D.; Merritt, D.M.; Pepin, D.M. Homogenization of regional river dynamics by dams and reservoirs on 21st-century rivers. *Proc. Natl. Acad. Sci. USA* **2007**, *104*, 5732–5737. [CrossRef] [PubMed]

Disclaimer/Publisher's Note: The statements, opinions and data contained in all publications are solely those of the individual author(s) and contributor(s) and not of MDPI and/or the editor(s). MDPI and/or the editor(s) disclaim responsibility for any injury to people or property resulting from any ideas, methods, instructions or products referred to in the content.